

# Prospects for Cosmology with Cluster Mass Profiles

Mary M. Crone<sup>1</sup>, Fabio Governato<sup>2</sup>, Joachim Stadel<sup>2</sup>, and Thomas Quinn<sup>2</sup>

## ABSTRACT

We test the precision with which weak lensing data can provide characteristic cluster mass profiles within Cold Dark Matter (CDM) scenarios. Using a parallel treecode to simulate volumes as large as  $500 h^{-1}$  Mpc with good resolution, we generate samples of large clusters within a standard CDM model and an open CDM model with  $\Omega_o = 0.3$ . We mock high-quality lensing data by including realistic errors, selecting cluster samples based on velocity dispersion, and fitting profiles within a realistic range in radius. We find that a sample of ten clusters can determine logarithmic profile slopes with  $1-\sigma$  errors of about 7%. Increasing the sample size to twenty brings this error down to less than 5%, but this is still insufficient to distinguish the two models. However, measures of cluster profiles obtained with weak lensing do place strong constraints for general CDM-like models of structure formation, and we discuss the optimal strategy for obtaining data samples to use for this purpose.

## 1. Introduction

Weak lensing of background galaxies provides a new method of mapping the mass distribution of galaxy clusters. Such data provide a particularly straightforward means of testing cosmological models, because they directly reflect the distribution of mass rather than that of galaxies or gas. Comparison to models is considerably further simplified if one uses *relative* mass profiles only, without requiring absolute mass normalization. Unlike absolute masses, relative densities can be obtained without mapping the cluster to high radii or knowing the redshifts of background galaxies (Kaiser & Squires 1993).

Cluster maps from weak lensing are collecting quickly thanks to wide-field CCDs, notably at the Canada-France-Hawaii Telescope. Nine clusters have published data. The outer radius covered is typically between  $500 h^{-1}$  kpc and  $1 h^{-1}$  Mpc (Smail *et al.* 1994, Fahlman *et al.* 1994, Squires *et al.* 1995, Seitz *et al.* 1996), but some data go as far as 1.5 or  $2.0 h^{-1}$  Mpc (Bonnet *et al.* 1994, Luppino & Kaiser 1996). Data for other clusters, some with radii out to  $2.0 h^{-1}$  Mpc, will be available soon (Squires, personal communication). Most of the clusters which have been mapped are very rich clusters at intermediate redshifts of about 0.2, with the notable exception of the high redshift cluster MS1054 (Luppino & Kaiser 1996). Profile fits are published for A1689

---

<sup>1</sup>Department of Physics & Astronomy, The University of Pittsburgh, Pittsburgh, PA 15260

<sup>2</sup> Astronomy Department, University of Washington, Seattle, WA 98195

(Tyson & Fischer), Cl 0024+1654 (Bonnet, Mellier, & Fort 1994), and 2218 (Squires *et al.* 1996). Logarithmic slopes for these clusters fall in the range 1.0 – 1.4.

The development of mass reconstruction algorithms with which to analyze these data is progressing as well. The standard method is that of Kaiser & Squires (1993), which uses the coherent shear of background galaxies. Recent work has improved upon this method (Bartelmann 1995, Seitz & Schneider 1996), and also provided alternatives, some of which include amplification as well as shear (Broadhurst *et al.* 1995, Van Waerbeke *et al.* 1996). An early study of the strengths and limitations of weak lensing analysis is that by Miralda-Escudé (1991); several more recent papers discuss the effects of seeing, noise, the limits of the weak lensing approximation, and contamination of the source field by cluster galaxies (Kaiser *et al.* 1995; Wilson *et al.* 1996, Squires *et al.* 1996). Another issue is the degree of lensing by large scale structure (Jaroszynsky *et al.* 1990, Watanabe & Tomita 1990, Blandford *et al.* 1991, Bartelmann & Schneider 1991, Kaiser 1992). In the context of mapping clusters, large scale structure introduces contamination in the outskirts of each cluster. Increased understanding of each of these issues will lead to more reliable mass maps, especially in the innermost and outermost regions of clusters.

Previous analytic and N-body studies predict that within hierarchical structure formation scenarios, cluster mass profiles depend on cosmological parameters (Hoffman & Shaham 1985; Crone, Evrard, & Richstone 1994). Specifically, if the initial mass density power spectrum is  $P(k) \propto k^n$ , higher values of the density parameter  $\Omega$  produce flatter profiles for a fixed value of the initial power index  $n$ . The situation is less clear for CDM models, which do not have pure power-law initial conditions; a recent study by Xu (1996) concludes that standard and low-density CDM models produce only slightly different profiles.

Profiles within CDM models are especially tricky to quantify because they themselves do not follow power laws, but have a significant curvature. Navarro, Frenk, & White (1996) show that when normalized to their virial radii, CDM clusters over a wide range in mass do have very similar shapes, on average. However, if the virial radius is unknown or only poorly known, as is the case for cluster observations, the curvature in CDM clusters means that the profile slope depends on the radial fitting region.

The purpose of this letter is to examine the precision with which weak lensing data can provide characteristic mass profiles within CDM models. We use large N-body simulations to produce a large number of clusters in two CDM models. We subsample and project each cluster to mock weak lensing data, and fit over a limited range in physical radius (in  $h^{-1}$  Mpc). We also assume rough knowledge of the cluster velocity dispersion. Intrinsic cluster-to-cluster variance, sampling error, and a dependence on the absolute cluster mass all limit the ability to determine precise characteristic profiles.

## 2. Methods and Results

We use simulations of two cosmological models, standard and open CDM, in two different volumes of space (see Table 1), for a total of four simulations. Using different volumes allows us to make predictions for clusters over a wide range in velocity dispersion. It also allows us to compare the two cosmologies using samples with the same velocity dispersion, because the open CDM (OCDM) model contains fewer massive clusters per comoving volume than the standard CDM (SCDM) model.

The simulations were generated by a parallel treecode with periodic boundary conditions (Stadel and Quinn 1997). They use a very large number of particles, as permitted by having a parallel code, and they have a rather small spline force softening. This permits us to resolve not only the central parts of each cluster, but also substructure and its effects on the evolution of the cluster profiles. A large softening (or, more generally, low resolution) can affect the shape of the cluster profiles by diminishing the maximum phase density actually resolved, thus prematurely erasing substructure falling into the cluster center (Moore *et al.* 1996). Timesteps were constrained to  $\Delta t < 0.3 \frac{\epsilon}{v_{max}}$ , where  $v_{max}$  is the approximate maximum speed and  $\epsilon$  is the softening length. The parameters of these simulations, including the density parameter  $\Omega_o$ , Hubble parameter  $H_o$ , the rms fluctuations on a scale of  $8h^{-1}$  Mpc ( $\sigma_8$ ), box length, number of particles  $N$ , and softening length are summarized in Table 1.

**TABLE 1**  
Simulation Parameters

Model	$\Omega_o$	$H_o$ ( $\frac{km/s}{Mpc}$ )	$\sigma_8$	length ( $h^{-1}Mpc$ )	$N$	$\epsilon$ ( $h^{-1}kpc$ )
SCDM (large)	1.0	50	0.7	500	$360^3$	50
(small)	1.0	50	0.7	50	$144^3$	30
OCDM (large)	0.3	75	1.0	500	$360^3$	63
(small)	0.3	75	1.0	75	$144^3$	45

### 2.1. The Cluster Sample

We identify clusters using a standard friends-of-friends algorithm, and select the twenty most massive clusters in each simulation. Clusters selected in this way span a wide range of dynamical states and morphologies, from relaxed and semi-isolated, to members of cluster associations of a few members. In each of the small volume simulations there is one cluster much larger than the others; we reject these clusters to produce samples which are more localized in velocity dispersion. The ranges in dispersion for each of these samples are 757 – 1098 km/s and 1827 – 2277 km/s

for SCDM, and  $419 - 674$  km/s and  $820 - 1082$  km/s for OCDM. The dispersions of the largest clusters in the large OCDM volume match those in the small SCDM volume, allowing us to compare dispersion-limited samples with clusters that are all well-resolved. Dispersion for clusters with weak lensing data currently range from 750 km/s (Fahlman *et al.* 1994) to 2000 km/s and even higher (Tyson, Valdes, & Wenk 1990), but are typically between 1000 km/s and 1500 km/s.

After selecting clusters from the N-body simulations, we need to project a three-dimensional region around each simulated cluster into two dimensions. To obtain an accurate profile we should include any structure in the cluster outskirts, the accumulated lensing of large-scale structure, and projections of other clusters along the line of sight. We find that structure in the immediate vicinity of the cluster is accounted for if we select a sphere out to an overdensity of five. (The profile slopes within our fitting region converge to a constant value at an overdensity greater than this.) The accumulated lensing from large-scale structure along the line of sight has been previously estimated to produce shear at the level of a few percent, and therefore to affect only the outskirts of clusters (see the references in §1). The influence of projected clusters and groups is discussed by Cen (1996), who concludes that much of the substructure associated with clusters can, especially in open models, be associated with spurious superpositions of clusters along the line of sight. We directly estimate whether cluster projections and large scale structure affect our profiles by cutting out cylinders (with length equal to that of the simulation volume) around a few clusters in each volume, and projecting these into two dimensions. A complete treatment of these projection effects involves propagating light rays through the entire distance between the source galaxies and the observer; here we test whether profiles are necessarily changed by structure within our simulation volumes of  $50 - 500 h^{-1}$  Mpc. We find that there is little effect on profile slopes within  $1 h^{-1}$  Mpc, the outer radius of the profile fitting region we use in this paper. In addition, problems introduced by superpositions on cluster *selection* can be alleviated by selecting from an X-ray catalog. Therefore, with a few caveats, we believe that we are able to obtain fairly accurate profiles for large clusters out to  $1/h^{-1}$  Mpc.

To obtain the two-dimensional density profiles, we identify cluster centers as the most bound particle in each cluster. Since we use no information at very small radii (less than  $0.15 h^{-1}$  Mpc), this choice is effectively equivalent to the two-dimensional density maximum for our purposes.

## 2.2. The Profile Fits

We find profiles for each individual cluster by averaging densities in bins of  $\log R (h^{-1} \text{Mpc}) = 0.1$ . If we use all the particles in each cluster, Poisson error in each bin is fairly small (between 2% and 8%). To mock lensing data, we subsample each bin to produce an error of 20%.

We characterize cluster mass profiles for each sample with a power-law fitting function within the region  $0.15 - 1.0 h^{-1}$  Mpc. The outer radial cutoff is motivated by constraints of telescope

time and the desire to avoid contributions from large-scale structure (as discussed above; also see Bonnet *et al.* 1994). The reliability of data at small radii is limited by contamination by cluster galaxies (that is, misidentification of cluster members as background source galaxies) and the need to remain at densities where the weak lensing approximation can be used. The inner cutoff of  $0.15 h^{-1}$  Mpc is a fairly optimistic estimate of the smallest radius at which reliable densities could be obtained for large clusters (Squires *et al.* 1996, Wilson *et al.* 1996).

Figure 1 shows a typical cluster profile, illustrating the quality of data we assume for our analysis. There is not enough information in each profile to use more complicated functions which describe CDM density profiles when all the information from simulations is used, such as a broken power-law or Hernquist function (Xu 1996, Navarro *et al.* 1996). Values of the reduced chi-squared indicate that a power law provides a good fit, except in some cases where substructure is clearly present.

We calculate characteristic profile slopes for samples of 10 and 20 clusters. For each sample, we draw 5000 bootstrap resamplings from our set of simulated clusters to estimate the mean profile and confidence levels. Figure 2 summarizes the power-law fits for each sample. For the large OCDM volume, we also show fits to each individual cluster (inset). Note the very wide range of values for individual clusters. The inset also illustrates that the variance within each sample is *not* caused by a velocity dispersion dependence; within each sample, there is no significant trend with velocity dispersion. The larger errors in the SCDM slopes is consistent with the fact that clusters in high- $\Omega$  models exhibit more local, (i.e. real) substructure (Crone, Evrard, & Richstone 1996). The intrinsic scatter in cluster profiles highlights the difficulty in drawing any conclusions based on small numbers, and it may severely affect measurements like the baryon abundance in clusters (see Loewenstein and Mushotzky, 1996). The error bars indicate  $1 - \sigma$  errors for the 10-cluster samples. Increasing the sample size to 20 decreases errors by about 30%, very close to the  $1/\sqrt{N}$  prediction from Gaussian statistics.

The most striking trend in Figure 2 is the dependence of slope on velocity dispersion. There are two causes for this. The primary one is that the profiles are not on average, pure power laws, so that the fixed physical range in radius used for the fit corresponds to a different region of the cluster depending on the cluster size. The other is that the profiles, even when rescaled to a characteristic radius, such as the virial radius, are intrinsically dependent on mass. Previous papers indicate that the second effect is quite small (Navarro *et al.* 1996, Xu 1996). We check this by fitting the 2000 km/s clusters to a new radial range determined by rescaling to approximate virial radii of the 900 km/s clusters. The new slope is consistent with that for the 900 km/s clusters in both models. Therefore, rescaling the fitting radius this way cannot be used to distinguish OCDM from SCDM, but the similarity of the two models, can be used to actually put a strong constraint on the whole class of CDM-like models.

If we compare the cluster samples in the 1000 km/sec velocity range (the only one in common between the two cosmological models and the simplest to assemble observationally), we find that

OCDM and SCDM cannot be distinguished at the  $2\sigma$  level, even using a 20-cluster sample.

We tried unsuccessfully to improve the cosmological signal at higher radii by fitting within the larger region  $0.15 - 2.0 h^{-1}$  Mpc. The logarithmic slopes systematically shift steeper by about 0.15, but the errors do not significantly decrease. This is not entirely surprising, because this is not a huge increase in logarithmic radius — the density changes by only a factor of two, and we gain only three data points. It may be possible to get better data within this range (at the expense of significant telescope time); for an even distribution of source galaxies and an isothermal profile, signal-to-noise is constant as a function of radius. However, it may not be worth the effort to do so (for this specific purpose) because both nearby substructure and intervening large-scale structure wreak havoc with the profiles at these relatively low overdensities. Also, it is more straightforward to compare fits which were made using constant error bars, because otherwise one region of the cluster is weighted more heavily than others.

This profile curvature suggests that it might be appropriate to attempt fitting to a more complicated function, if not for each individual cluster, for an average profile for the sample. However, we find that for these samples the errors in such multi-parameter fits are large enough that it is more useful to use a simple power law.

### 3. Discussion

Within the CDM models considered here, a sample of ten clusters with high-quality lensing data can determine logarithmic profile slopes with  $1\sigma$  errors of about 7%. Increasing the sample size to twenty lowers the errors to about 5%. This is insufficient to distinguish the models, and additional data at larger radii do not help. Nevertheless, profiles for samples this large put a strong constraint on CDM models as a whole, independently of the particular model adopted. This is especially important as recent data challenge not only the SCDM model (Loewenstein & Mushotzky, 1996) but the whole class of CDM-like models (Davis *et al.* 1992, White *et al.* 1993). Moreover cluster profiles have the major advantage of not requiring any absolute mass normalization and are easily obtainable with present day telescopes.

We find that it is crucial to perform fits within a consistent radial range, and to use a cluster sample within a limited range in velocity dispersion. This is because the profiles are not exact power laws, so that a fixed aperture corresponds to a different characteristic region of the cluster, depending on its size. Another point to consider is that clusters with lensing data are scattered over a range of redshift space, while our simulated clusters are at  $z = 0$ , although significant evolution is not expected (Xu 1996).

Although this study was designed with weak lensing data in mind, the results can also be compared with other measures of cluster profiles, such as X-ray maps and galaxy distributions (for example, Lubin & Postman 1996). We conclude that an ideal observational program should involve cluster selection using an X-ray catalogue (Luppino & Gioia 1994), with further cuts to

roughly limit the sample in both redshift and velocity dispersion. Such data would also form a base for systematic studies of mass-to-light ratios and substructure, providing powerful and direct constraints on the structure of clusters (Wilson, Cole & Frenk 1996b).

We thank George Lake, Gordon Squires, and Gus Evrard for useful discussions. The simulations were performed at the ARSC, NCSA, PSC, and CTC supercomputing centers. This research was funded by the NASA HPCC/ESS program.

## REFERENCES

Bartelmann, M. 1995, *A&A*, 303, 643  
Bartelmann, M. & Schneider, P. 1991, *A&A*, 248, 349  
Bartelmann, M. & Steinmetz, M. 1996, *astro-ph/9603101*  
Blandford, R.D., Saust, A.B., Brainerd, T.G., Villumsen, J. 1991, *MNRAS*, 251, 600  
Bonnet, H., Mellier, Y., & Fort, B. 1994, 427, L83  
Broadhurst, T.J., Taylor, A.N. & Peacock, J.A. 1995, *ApJ*, 438, 49  
Cen, R. 1996, *astro-ph/9608070*  
Crone, M.M., Evrard, A.E. & Richstone, D.O. 1994, *ApJ*, 434, 402  
Crone, M.M., Evrard, A.E. & Richstone, D.O. 1996, *ApJ*, in press  
Davis, M., Efstathiou, G., Frenk, C.S., & White, S.D.M. 1992, *Nature*, 356, 489  
Edge, A.C. & Stewart, G.C. 1991, *MNRAS*, 252, 428  
Fahlman, G., Kaiser, N., Squires, G., Woods, D. 1994, 437, 56  
Hoffman, Y., & Shaham, J. 1985, *ApJ*, 297, 16  
Jaroszyński, M., Park, C., Paczyński, & Gott, J.R. 1990, *ApJ*, 365, 22  
Kaiser, N. 1992, *ApJ*, 388, 272  
Kaiser, N. & Squires, G. 1993, *ApJ*, 404, 441  
Kaiser, N., Squires, G., & Broadhurst, T. 1995, *ApJ*, 449, 460  
Kneib, J.-P., Ellis, R.S., Smail, I., Couch, W.J., & Sharples, R.M. 1995, *astro-ph/9511015*  
Loewenstein, M. & Mushotzky, R.F. 1996, *astro-ph/9608111*  
Lubin, L.M. & Postman, M. 1996, *astro-ph/9602013*  
Luppino, G.A. & Gioia, I.M. 1994, *ApJS*, 94, 583  
Miralda-Escudé, J. 1991, *ApJ*, 370, 1  
Mohr, J.J., Fabricant, D.G., & Geller, M.J. 1993, *ApJ*, 413, 492  
Moore, B., Katz, N. & Lake, G. 1996, *ApJ*, 457, 455  
Navarro, J.F., Frenk, C.S., & White, S.D.M. 1996, *ApJ*, 462, 563  
Seitz, S. & Schneider, P. 1996, *A&A*, 305, 383  
Smail, I. & Dickinson, M. 1995, *ApJ*, 455, L99  
Smail, I., Ellis, R.S., & Fitchett, M.J. 1995, *MNRAS*, 273, 277

Smail, I., Ellis, R.S., & Fitchett. M.J., & Edge, A. 1994,  
Squires, G., Neumann, D.M., Kaiser, N., Arnaud, M., Babul, A., Bohringer, H., Fahlman, G., &  
Woods, D. 1996, astro-ph/9603050  
Squires, G., Kaiser, N., Babul, A., Fahlman, G., Woods, D., Neumann, D.M., & Boehringer, H.  
1996, ApJ, 461, 572  
Squires, G., Kaiser, N., Fahlman, G., Babul, A., & Woods, D., 1996, astro-ph/9602105  
Stadel, J., and Quinn, T. 1997, in preparation  
Tyson, J.A. & Fischer, P. 1995, ApJ, 446, L55  
Tyson, J.A., Valdes, F., & Wenk, R.A. 1990, ApJ, 349, L1  
Van Waerbeke, L., Mellier, Y., Schneider, P., Fort, B., Mathez, G 1996, A&A, in press  
Waxman, E., Miralda-Escudé, J. 1995, ApJ, 451, 451  
White, S.D.M., Efstathiou, G., & Frenk, C.S. 1993, MNRAS, 262, 1023  
White, S.D.M., Navarro, J.F., Evrard A. & Frenk, C.S. 1993, Nature, 366, 429  
Wilson, G., Cole, S., & Frenk, C.S. 1996, MNRAS, 280, 199  
Wilson, G., Cole, S., & Frenk, C.S. 1996b, MNRAS, 282, 501  
Xu, G. 1996, preprint

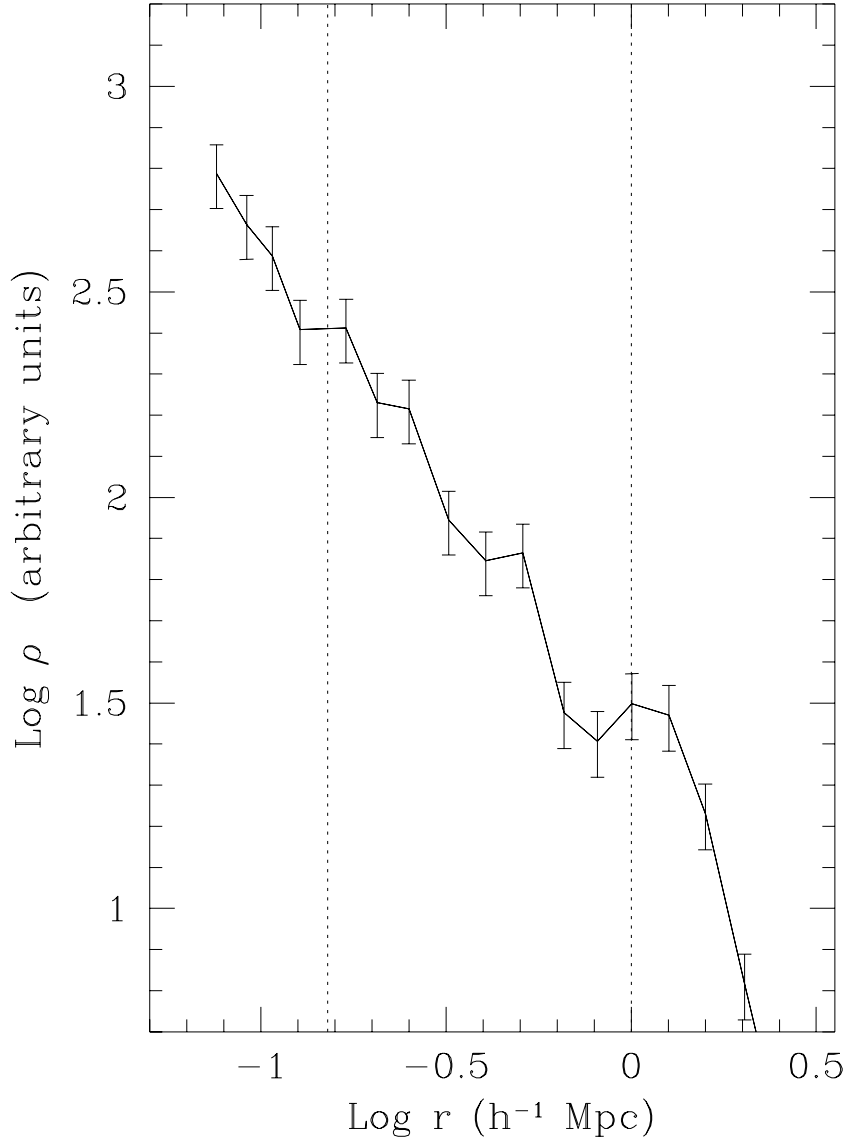


Fig. 1.— A typical profile within the SCDM model, illustrating the quality of data we assume for our analysis. Dotted vertical lines indicate the radial region within which we perform our fits:  $0.15 - -1.0 h^{-1}$  Mpc. Power laws provide good fits to the cluster profiles, except in some cases where substructure is clearly present.

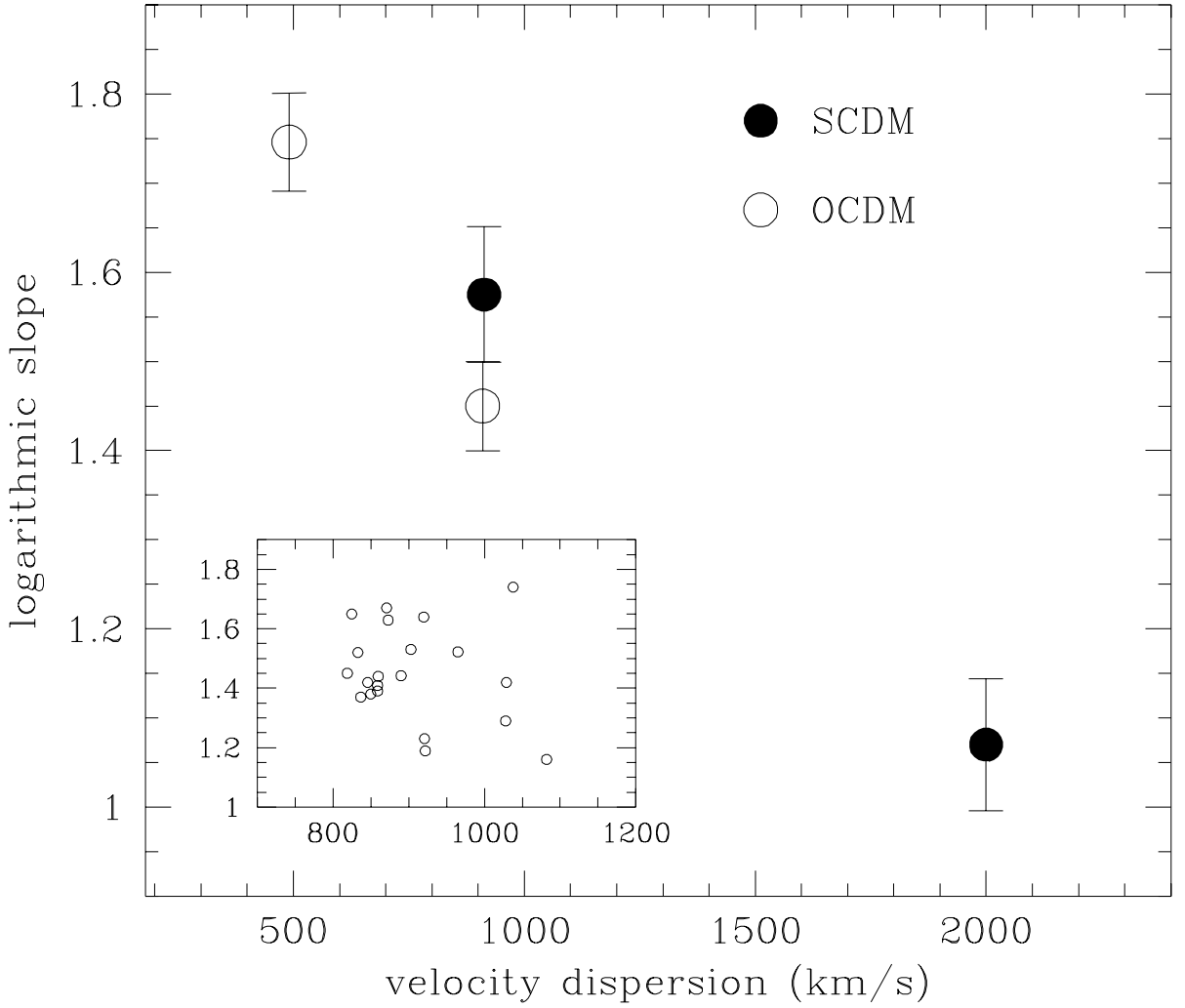


Fig. 2.— Best fit power-law slopes versus the average one-dimensional velocity dispersion of each sample, in the radial range  $0.15 - 1.0 h^{-1}$  Mpc. We also show slopes and velocity dispersions for each individual cluster in the sample of larger OCDM clusters (inset). The range of dispersions for each sample is given in the text. All error bars indicate  $1 - \sigma$  errors for the 10-cluster samples.